pH-Dependent pK_a Values in Proteins—A Theoretical Analysis of Protonation Energies with Practical Consequences for Enzymatic Reactions

Elisa Bombarda and G. Matthias Ullmann*

Structural Biology/Bioinformatics, University of Bayreuth, Universitätsstrasse 30, BGI, 95447 Bayreuth, Germany

Received: September 15, 2009

Because of their central importance for understanding enzymatic mechanisms, pK_a values are of great interest in biochemical research. It is common practice to determine pK_a values of amino acid residues in proteins from NMR or FTIR titration curves by determining the pH at which the protonation probability is 50%. The pH dependence of the free energy required to protonate this residue is then determined from the linear relationship $\Delta G_{prot} = RT \ln 10\ (pH - pK_a)$, where R is the gas constant and T the absolute temperature. However, this approach neglects that there can be important electrostatic interactions in the proteins that can shift the protonation energy. Even if the titration curves seem to have a standard sigmoidal shape, the protonation energy of an individual site in a protein may depend nonlinearly on pH. To account for this nonlinear dependence, we show that it is required to introduce pK_a values for individual sites in proteins that depend on pH. Two different definitions are discussed. One definition is based on a rearranged Henderson−Hasselbalch equation, and the other definition is based on an equation that was used by Tanford and Roxby to approximate titration curves of proteins. In the limiting case of weak interactions, the two definitions lead to nearly the same pK_a value. We discuss how these two differently defined pK_a values are related to the free energy change required to protonate a site. Using individual site pK_a values, we demonstrate on simple model systems that the interactions between protonatable residues in proteins can help to maintain the energy required to protonate a site in the protein nearly constant over a wide pH range. We show with the example of RNase T1 that such a mechanism to keep the protonation energy constant is used in enzymes. The pH dependence of pK_a values may be an important concept in enzyme catalysis. Neglecting this concept, important features of enzymes may be missed, and the enzymatic mechanism may not be fully understood.

Introduction

The knowledge of pK_a values of residues in proteins is essential for understanding protein function. On one hand, the pK_a value determines the protonation and thus the charge of a residue at a given pH. This information is important for rationalizing the interaction between proteins. On the other hand, the pK_a value determines the energy required to protonate or deprotonate a group, information that is often necessary to describe enzymatic mechanisms or proton transfer processes. Thus, when discussing enzymatic mechanisms, the question "What is the pK_a value of a group?" implicitly asks "What is the energy required to deprotonate a group?". For an isolated protonatable group, the pK_a value is proportional to the standard free energy of protonation $\Delta G^{o}_{prot} = -RT \ln 10\ pK_a$ (i.e., at standard condition pH = 0) where R is the gas constant and T the absolute temperature. A linear equation relates the free energy of protonation to the pK_a value of the group and the pH value of the solution (see Figure 1).

$$\Delta G_{prot} = RT \ln 10\ (pH - pK_a) \qquad (1)$$

When the pK_a value of a group is known, eq 1 is used to see how easy it is to protonate or deprotonate that group at a given pH. The smaller the absolute value of the difference between the pK_a and the solution pH, the easier it is to change the protonation state.

In proteins, protonatable residues can be rarely separated from each other. They mutually interact more or less strongly. A sign of this interaction is that titration curves of amino acids in proteins are often flatter than standard Henderson−Hasselbalch curves[1] or show even an irregular shape.[2−4] It follows that half-points (pH at which the protonation probability is 50%, also called p$K_{1/2}$) or inflection points of titration curves are not appropriate to determine the pK_a value of a site in a protein.[5−7] Often however, amino acid residues in proteins may titrate with an apparently standard Henderson−Hasselbalch curve.[4] In this case, it may appear at a first look appropriate to use the inflection point of this titration curve as the pK_a value of the residue in the protein. Anyway, this approach is not necessarily correct as we will demonstrate.

In this paper, we will discuss two definitions of pK_a values of individual sites in proteins and their relation to protonation energies. We will demonstrate that these pK_a values are pH dependent, since the protonation energies of these sites do not depend linearly on pH. Due to the interaction of several titratable sites, the protonation energy of sites in proteins can remain nearly constant over a wide pH range. It is important to realize that this behavior cannot be described by a single, pH-independent pK_a value.

* To whom correspondence should be addressed. E-mail: Matthias.Ullmann@uni-bayreuth.de.

10.1021/jp908926w
Published on Web 01/20/2010

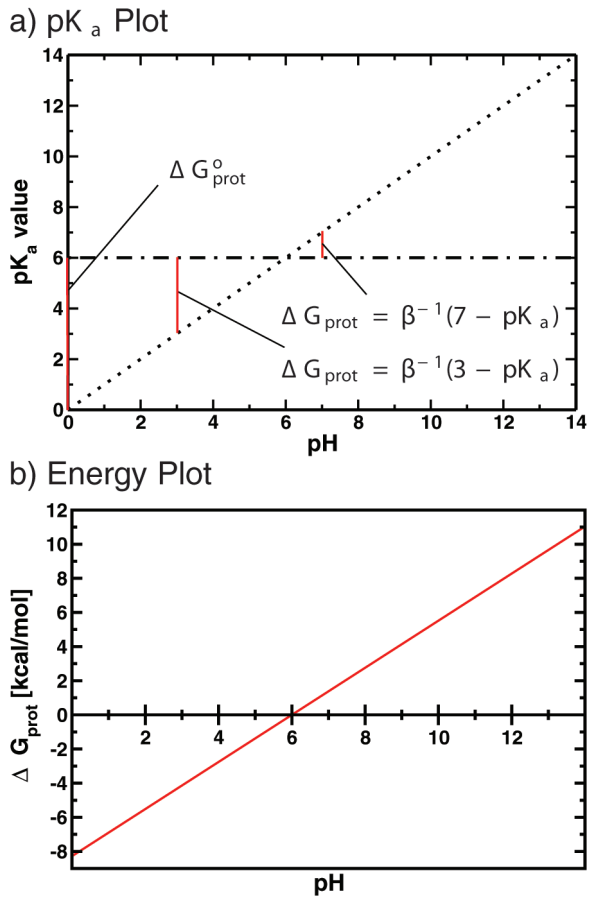

Figure 1. pK_a plot and protonation energy plot (eq 1) of an isolated titratable site. (a) pK_a plot of an isolated group with pK_a = 6.0 (dashed-dotted curves parallel to the *x*-axis). The dotted curve is the line where pK_a = pH. The red bars (here at pH 0, 3, and 7) symbolize the energy difference for protonating a site at a given pH (in pK_a units). (b) Protonation energy plot of an isolated group with pK_a = 6.0. The red line is obtained by plotting the values corresponding to the red bars in the pK_a plot. This free energy depends linearly on pH. The protonation energy is zero when pK_a = pH.

Theory

Protonation Equilibria of Proteins. ***Microstate Model.*** We consider a protein with N protonatable sites. Assuming that each site can exist in two forms (protonated and deprotonated), such a protein can adopt $M = 2^N$ states. Each state of the system can be written as an N-dimensional vector $\vec{x}_\nu = (x_{\nu,1}, ..., x_{\nu,N})$, where $x_{\nu,i}$ is 0 or 1 when site i is deprotonated or protonated, respectively. The Greek letter ν will be used as state index and the roman letters i and j will be used as site indices. Compared to an arbitrarily defined reference state $\vec{x}_\nu^\circ$ with the energy 0, each state $\vec{x}_\nu$ of the system has a well-defined energy E_ν which depends on the protonation energy of the individual proton binding sites (see eq 1) and the interaction between these sites

$$E_\nu = \sum_{i=1}^{N} (x_{\nu,i} - x_i^\circ) RT \ln 10\,(\mathrm{pH} - \mathrm{p}K_{\mathrm{intr},i}) + \sum_{i=1}^{N}\sum_{j<i}^{N} (x_{\nu,i} - x_i^\circ)(x_{\nu,j} - x_j^\circ) W_{ij} \quad (2)$$

where R is the gas constant, T is the absolute temperature, $x_{\nu,i}$ denotes the protonation form of the site i in state $\vec{x}_\nu$ and x_i° is the reference form of site i, pH is the pH value of the solution, p$K_{\mathrm{intr},i}$ is the pK_a value that site i would have if all other sites are in their reference form (intrinsic pK_a value), and W_{ij} represents the interaction between site i and site j. The energetic parameters p$K_{\mathrm{intr},i}$ and W_{ij} can be calculated using electrostatic methods.[8−11] If conformational changes need to be considered, eq 2 will assume a more complicated expression. However, since fundamental features are already captured by this form of eq 2, this expression will be used in this paper without losing generality. If more complicated expressions are necessary, the required modifications of the formalism are straightforward.

The p$K_{\mathrm{intr},i}$ value of an amino acid residue in the protein can be shifted compared to the value of an appropriate model compound in aqueous solution due to two effects. First, the protonatable site can be more or less buried in the protein which causes a desolvation of the proton binding site. This desolvation leads to a destabilization of the charged form of the site. Second, nontitrating charges and dipoles of the protein may interact with the proton binding site. Depending on the kind of interaction, this effect may stabilize either the charged form or the uncharged form.

The probability P_ν of protonation state ν in thermodynamic equilibrium can be calculated from the energies of all the states of the system

$$P_\nu^{\mathrm{eq}} = \frac{\mathrm{e}^{-\beta E_\nu}}{Z} \quad (3)$$

with $\beta = 1/(RT)$ and Z being the partition function of the system.

$$Z = \sum_{\nu=1}^{M} \mathrm{e}^{-\beta E_\nu} \quad (4)$$

The sum runs over all M possible states. The equilibrium protonation probability $\langle x_i \rangle$ of site i in the protein, i.e., its titration curve, is given by

$$\langle x_i \rangle = \sum_{\nu}^{M} x_{\nu,i} P_\nu^{\mathrm{eq}} \quad (5)$$

where $x_{\nu,i}$ denotes the protonation form of site i in the protonation state $\vec{x}_\nu$. The probability of being deprotonated is given by

$$1 - \langle x_i \rangle = \sum_{\nu}^{M} (1 - x_{\nu,i}) P_\nu^{\mathrm{eq}} \quad (6)$$

For small systems, this sum can be evaluated explicitly. For larger systems, Monte Carlo techniques can be used to determine these probabilities.[12]

Protonation Equilibrium Constants in Proteins. When many protons can bind to one protein, one can differentiate between macroscopic and microscopic protonation constants.[13,6] The nth macroscopic protonation constant defines the equilibrium between all states that have n and $(n - 1)$ protons bound. There are in total as many macroscopic protonation constants as there are proton binding sites in the protein. However, an assignment of a macroscopic protonation constant to an individual site is in principle not possible.

Microscopic protonation constants describe the equilibrium between two protonation states that differ in the protonation of one site while the remaining sites do not change their protonation. In a protein with N proton binding sites, there are $N2^{N-1}$ microscopic protonation constants of which only $2^N - 1$ are independent of each other.[6] For each site, there are 2^{N-1} microscopic protonation constants which can differ significantly depending on the interaction between the sites. The microscopic pK_a values can be calculated from the energy difference of the two respective microstates. Using eq 2, one obtains

$$\mathrm{p}K_{\nu,i} = \mathrm{p}K_{\mathrm{intr},i} - \sum_{j=1}^{N} (x_{\nu,j} - x_j^\circ) W_{ij} \tag{7}$$

Microscopic pK_a values can be assigned to individual sites. However, since for each site there are 2^{N-1} microscopic constants, a single microscopic pK_a value does not describe the protonation of a site appropriately over the whole pH range.

Defining pK_a Values of Individual Sites in Proteins. In order to characterize the protonation behavior of an individual site of a protein, it is desirable to define a single pK_a value that can be uniquely assigned to that site. However, such a definition is not straightforward and deserves some reflection. Two definitions seem physically meaningful to us.

Tanford−Roxby pK_a Value. A possible definition of the pK_a value of an individual site can be an average microscopic pK_a value. In analogy to the average protonation probability of a site (eq 5), an average microscopic pK_a value can be defined as

$$\langle \mathrm{p}K_i \rangle = \sum_{\nu}^{M} \mathrm{p}K_{\nu,i} P_\nu^{\mathrm{eq}} \tag{8}$$

P_ν^{eq} is the probability of state ν as defined in eq 3. Thus, eq 8 can be rewritten as

$$\langle \mathrm{p}K_i \rangle = \frac{\sum_{\nu=1}^{M} \mathrm{p}K_{\nu,i} \mathrm{e}^{-\beta E_\nu}}{\sum_{\nu=1}^{M} \mathrm{e}^{-\beta E_\nu}} \tag{9}$$

With eq 7 in eq 9, we obtain

$$\langle \mathrm{p}K_i \rangle = \frac{\sum_{\nu=1}^{M} (\mathrm{p}K_{\mathrm{intr},i} - \sum_{j=1}^{N} (x_{\nu,j} - x_j^\circ) W_{ij}) \mathrm{e}^{-\beta E_\nu}}{\sum_{\nu=1}^{M} \mathrm{e}^{-\beta E_\nu}} \tag{10}$$

$$= \frac{\sum_{\nu=1}^{M} \mathrm{p}K_{\mathrm{intr},i} \mathrm{e}^{-\beta E_\nu} - \sum_{\nu=1}^{M} \mathrm{e}^{-\beta E_\nu} (\sum_{j=1}^{N} (x_{\nu,j} - x_j^\circ) W_{ij})}{\sum_{\nu=1}^{M} \mathrm{e}^{-\beta E_\nu}} \tag{11}$$

Interestingly using eqs 7 and 5, it can be shown that eq 8 is equivalent to eq 12, which was proposed by Tanford and Roxby to calculate the protonation behavior of a protein in an iterative scheme.[14]

$$\langle \mathrm{p}K_i \rangle = \mathrm{p}K_{\mathrm{TR},i} = \mathrm{p}K_{\mathrm{intr},i} - \sum_{j=1}^{N} (\langle x_j \rangle - x_j^\circ) W_{ij} \tag{12}$$

The protonation probability of site i is given by eq 5. If we use eq 5 in eq 12, we get

$$\langle \mathrm{p}K_i \rangle = \mathrm{p}K_{\mathrm{intr},i} - \sum_{j=1}^{N} \left(\frac{\sum_{\nu=1}^{M} x_{\nu,i} \mathrm{e}^{-\beta E_\nu}}{\sum_{\nu=1}^{M} \mathrm{e}^{-\beta E_\nu}} - x_j^\circ \right) W_{ij} \tag{13}$$

$$= \frac{\sum_{\nu=1}^{M} \mathrm{p}K_{\mathrm{intr},i} \mathrm{e}^{-\beta E_\nu} - \sum_{\nu=1}^{M} \sum_{j=1}^{N} (x_{\nu,i} - x_j^\circ) W_{ij} \mathrm{e}^{-\beta E_\nu}}{\sum_{\nu=1}^{M} \mathrm{e}^{-\beta E_\nu}} \tag{14}$$

$$= \frac{\sum_{\nu=1}^{M} \mathrm{p}K_{\mathrm{intr},i} \mathrm{e}^{-\beta E_\nu} - \sum_{\nu=1}^{M} \mathrm{e}^{-\beta E_\nu} (\sum_{j=1}^{N} (x_{\nu,i} - x_j^\circ) W_{ij})}{\sum_{\nu=1}^{M} \mathrm{e}^{-\beta E_\nu}} \tag{15}$$

One can see that eq 15 and eq 11 are identical, which means that the Tanford−Roxby-pK_a value defines an average microscopic pK_a value of site i. Because of this equivalence, the average microscopic pK_a value $\langle \mathrm{p}K_i \rangle$ will be called Tanford−Roxby (TR) pK_a value (p$K_{\mathrm{TR},i}$).[15] The summation in eq 12 gives the average interaction energy with the other sites of the protein, which depends on the average protonation probability $\langle x_j \rangle$ of the sites and thus on pH. However, it is not considered that also other sites can change their equilibrium protonation probability when site i changes its protonation.

Henderson−Hasselbalch pK_a Value. An alternative definition of the pK_a value of an individual site can be obtained by rearranging the Henderson−Hasselbalch equation:

$$\mathrm{p}K_{\mathrm{HH},i} = \mathrm{pH} + \log_{10}\left(\frac{\langle x_i \rangle}{1 - \langle x_i \rangle} \right) \tag{16}$$

We call this pK_a value Henderson−Hasselbalch (HH) pK_a value (p$K_{\mathrm{HH},i}$). It can be shown that with this definition, the pK_a values relates to a free energy difference. The free energy of a system is generally defined by $G = -RT \ln Z$, where Z is the partition function defined in eq 4. Thus, the free energy for protonating a site is given by

$$\Delta G_{\mathrm{prot},i} = -RT(\ln Z_{\mathrm{prot},i} - \ln Z_{\mathrm{deprot},i}) \tag{17}$$

Based on eq 1, we can define the pK_a value of site i as

$$pK_i = pH - \frac{\Delta G_{prot,i}}{RT \ln 10} \quad (18)$$

Using eqs 4 and 17, one obtains from eq 18

$$pK_i = pH + \frac{1}{\ln 10}(\ln(\sum_{\nu=1}^{M} x_{\nu,i} e^{-\beta E_\nu}) - \ln(\sum_{\nu=1}^{M} (1 - x_{\nu,i}) e^{-\beta E_\nu})) \quad (19)$$

The two factors $x_{\nu,i}$ and $(1 - x_{\nu,i})$ are filters that cancel all terms from the partition function (eq 4) in which site i is deprotonated or protonated, respectively. Adding the constant term $-\ln \sum_{\nu=1}^{M} e^{-\beta E_\nu}$ to both logarithmic terms, one obtains

$$pK_i = pH + \frac{1}{\ln 10}\left(\ln \frac{\sum_{\nu=1}^{M} x_{\nu,i} e^{-\beta E_\nu}}{\sum_{\nu=1}^{M} e^{-\beta E_\nu}} - \ln \frac{\sum_{\nu=1}^{M} (1 - x_{\nu,i}) e^{-\beta E_\nu}}{\sum_{\nu=1}^{M} e^{-\beta E_\nu}} \right) \quad (20)$$

By considering the definition of the probability (eq 3), eq 20 becomes

$$pK_i = pH + \frac{1}{\ln 10}(\ln(\sum_{\nu=1}^{M} x_{\nu,i} P_\nu^{eq}) - \ln(\sum_{\nu=1}^{M} (1 - x_{\nu,i}) P_\nu^{eq})) \quad (21)$$

Applying a logarithmic law

$$pK_i = pH + \frac{1}{\ln 10}\left(\ln \frac{\sum_{\nu=1}^{M} x_{\nu,i} P_\nu^{eq}}{\sum_{\nu=1}^{M} (1 - x_{\nu,i}) P_\nu^{eq}} \right) \quad (22)$$

and considering eqs 5 and 6, we finally obtain

$$pK_i = pH + \frac{1}{\ln 10}\left(\ln \frac{\langle x_i \rangle}{1 - \langle x_i \rangle} \right) \quad (23)$$

As one can see, eq 18, which relates the pK_a value to a free energy change, is equivalent to the rearranged Henderson−Hasselbalch equation (eq 16). With this definition, the pH dependence of the interactions with other residues as well as changes in average protonation probabilities of the other sites are considered explicitly.

Meaning of the pK_a Values of Individual Sites. Obviously, the two definitions in eq 8 and eq 16 are not equivalent. For weak interactions, the difference between the two definitions is almost negligible; instead, for strong interactions, the difference is significant. However, both definitions are meaningful, since they describe different limiting scenarios. The physical picture that is connected to the TR-pK_a value (eq 8) describes a situation in which the protonation of all sites is in equilibrium with the solution $(\langle x_1 \rangle, ..., \langle x_i \rangle, ..., \langle x_N \rangle)_{eq}$. As depicted in eq 24, the protonation of site i is changed from 1 to 0, while all other sites maintain the average protonation that they have in equilibrium.

$$(\langle x_1 \rangle, ..., 1, ..., \langle x_N \rangle) \rightarrow (\langle x_1 \rangle, ..., 0, ..., \langle x_N \rangle) \quad (24)$$

This picture implies that the deprotonation of site i is faster than the equilibration of the protonation of the surrounding residues. This scenario could be relevant for acid base catalysis when a residue of the active site transiently takes a proton from the substrate, but the other residues do not have time to re-equilibrate their protonation.

The physical picture that is connected to the HH-pK_a value (eq 16) is related to the free energy difference of protonation. The reaction starts from a situation in which site i is protonated and all other sites adapt to this protonation and ends with site i deprotonated and again all other sites adapt to the situation (eq 25).

$$(\langle x_1 \rangle', ..., 1, ..., \langle x_N \rangle')_{eq,p} \rightarrow (\langle x_1 \rangle'', ..., 0, ..., \langle x_N \rangle'')_{eq,d} \quad (25)$$

In this scenario, the deprotonation of site i is considered to be slow enough to allow all other residues to equilibrate before and after deprotonation.

In contrast to microscopic and macroscopic pK_a values which do not depend on pH, both definitons of the individual site pK_a value lead to pH-dependent pK_a values. The reason for this pH dependence is that the interaction between the sites depends on pH, since the charge of the sites depends on pH. Moreover, in the case of the HH-pK_a value, the number of protons bound to the protein before and after the deprotonation reaction does not necessarily differ by exactly one. From the pH dependence of the two definitions of the individual site pK_a values, one can thus conclude that the deprotonation energy of a residue inside a protein does not depend linearly on pH in contrast to the case when pH-independent pK_a values are considered.

Methods

Structure Preparation. For the electrostatic calculations, the structures of spinach plastocyanin (PDB code 1AG6)[16] and RNase T1 (PDB code 1BVI, chain A)[17] were used. The guanosine-2′-monophosphate bound to RNase T1 was deleted from the structure. Hydrogens were added to the structure using the program CHARMM.[18] The positions of the hydrogens were energetically minimized, while the positions of all non-hydrogen atoms were kept fixed. After energy minimization, the water molecules were deleted from the structure.

Continuum Electrostatics Calculations. The intrinsic pK_a value (p$K_{a,i}^{intr}$) for each titratable site and the interaction energies between them (the W_{ij} site−site interactions) in eq 2 were obtained by continuum electrostatics calculations.[8] The Poisson−Boltzmann equation was solved by a finite-difference method using the MEAD program suite.[19] All aspartate, histidine, glutamate, lysine, arginine, and tyrosine residues were considered as protonatable sites. Atomic partial charges for standard amino acid groups were taken from the CHARMM22 parameter set.[20] The pK_a values of the model compounds were taken from the literature.[1,10] The dielectric constant of the protein was set to 4, and that of the solvent was set to 80. The dielectric boundary between solute and solvent was calculated using a water probe sphere of 1.4 Å radius and the atomic radii (1.0 Å for H, 1.55 Å for N, 1.7 Å for C, 1.5 Å for O, and 1.8 Å for S). The ionic strength was set to 0.1 M. The thickness of the ion exclusion layer was set to 2.0 Å.

Continuum electrostatics calculations were performed using the focusing technique[21] in two steps using a grid with 81^3

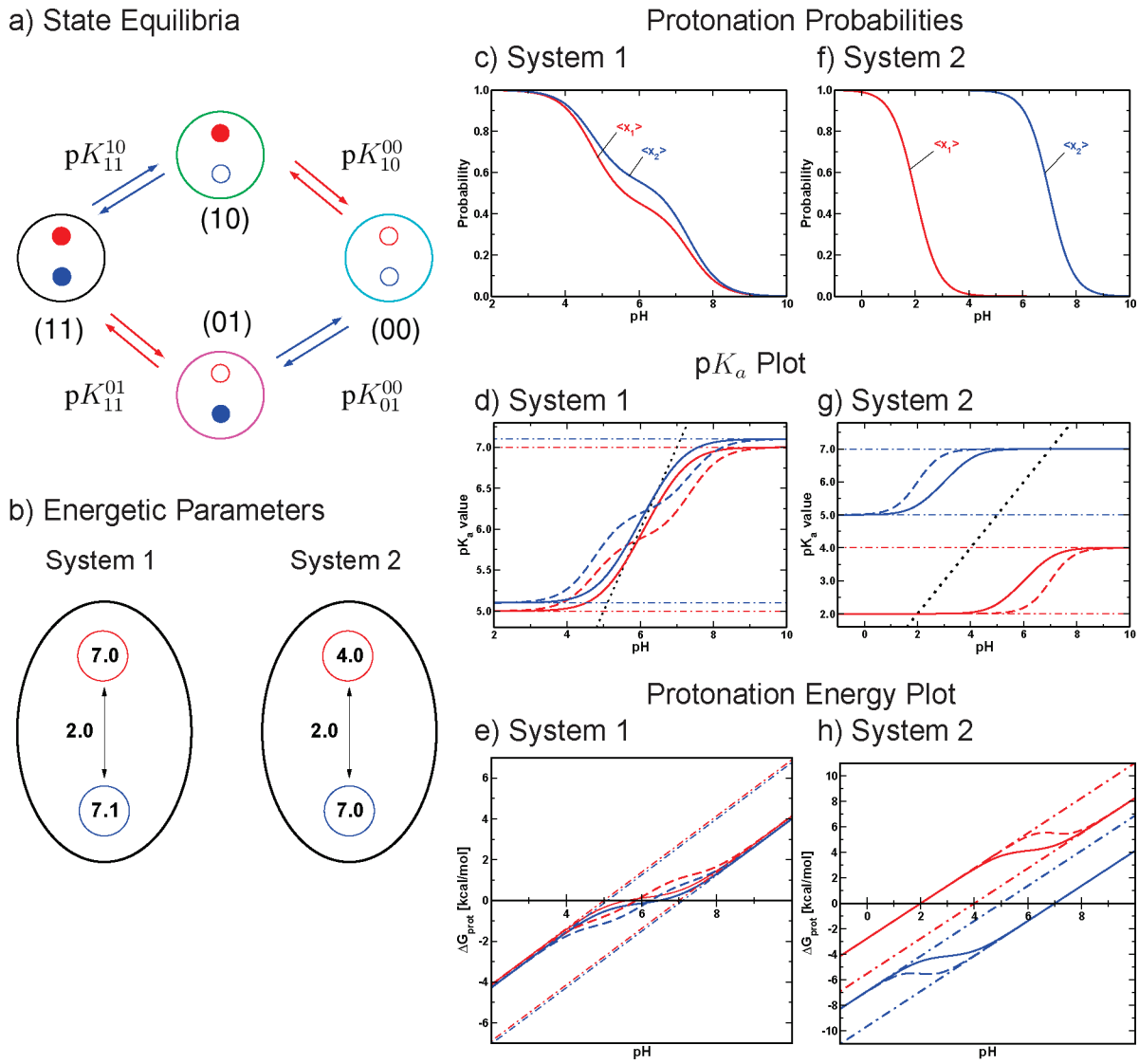

Figure 2. (a) State equilibria of a system with two titratable sites. Four protonation microstates exist for such a system. The protonation state vectors are given in parentheses. (b) Energetic parameters of the two discussed systems. The numbers inside the circles give the pK_{intr} values, and the numbers at the arrows give the interaction energy of the protonated species in pK_a units. (c) Titration curves of the individual sites (protonation probabilities) for system 1. (d) Differently defined pK_a values for the two sites of systems 1: HH-pK_a (solid), TR-pK_a (dashed), microscopic pK_a (dashed-dotted), and the bisection line pH = pK_a (dotted line). (e) Protonation free energies for system 1 calculated from eq 1 for the differently defined pK_a values (same coding as above). (f) Titration curves of the individual sites (protonation probabilities) for system 2. (g) Differently defined pK_a values for the two sites of system 2; the lines have the same meaning as in (d). (h) Protonation free energies for system 2 calculated from eq 1 for the differently defined pK_a values (same coding as above). The colors in all graphs and schemes are associated with the corresponing sites (red for site 1; blue for site 2).

points. The outer grid had a grid spacing of 1.0 Å and was placed at the geometric center of the protein. The inner grid had a grid spacing of 0.25 Å and was centered at the titratable site. A similar procedure was used for the model compound, with all grids centered at the titratable site.

Results and Discussions

Illustrative Examples. In order to illustrate the meaning of individual site pK_a value on some examples, we will discuss first a system of two and then of three interacting sites. In addition, we will discuss two real examples of proteins: the titration behavior of residues in electron transfer protein plastocyanin[22] and in the enzyme RNase T1.[23] The practical importance of individual site pK_a values will become evident from these examples.

System with Two Sites. Let us consider a system with only two interacting protonatable sites as depicted in Figure 2. For convenience, we choose the sites to be cationic in the protonated form, and the fully deprotonated state is taken as the reference state. The interaction energy between the two sites is set to 2.0 pK_a units when they are protonated and otherwise to zero. An interaction energy of 2.0 pK_a units and more can be found frequently in proteins.[12,24,25]

First, we consider two interacting sites that titrate in the same pH range; i.e., their titration curves overlap (system 1 in Figure 2). We set the intrinsic pK_a values to 7.0 and 7.1, which due to the interaction energy of 2.0 pK_a units results in the following microscopic pK_a values: $pK_1^{10} = 5.1$, $pK_1^{01} = 5.0$, $pK_{01}^{00} = 7.1$, and $pK_{10}^{00} = 7.0$. The subscripts and superscripts of the pK_a values indicate the reactant and product state vectors, respectively. As discussed in previous publications,[6,7] the individual titration curves of the two sites can become irregular under these circumstances. From the titration curves (Figure 2c), one can read half-protonation points (often called p$K_{1/2}$ values) of 5.6

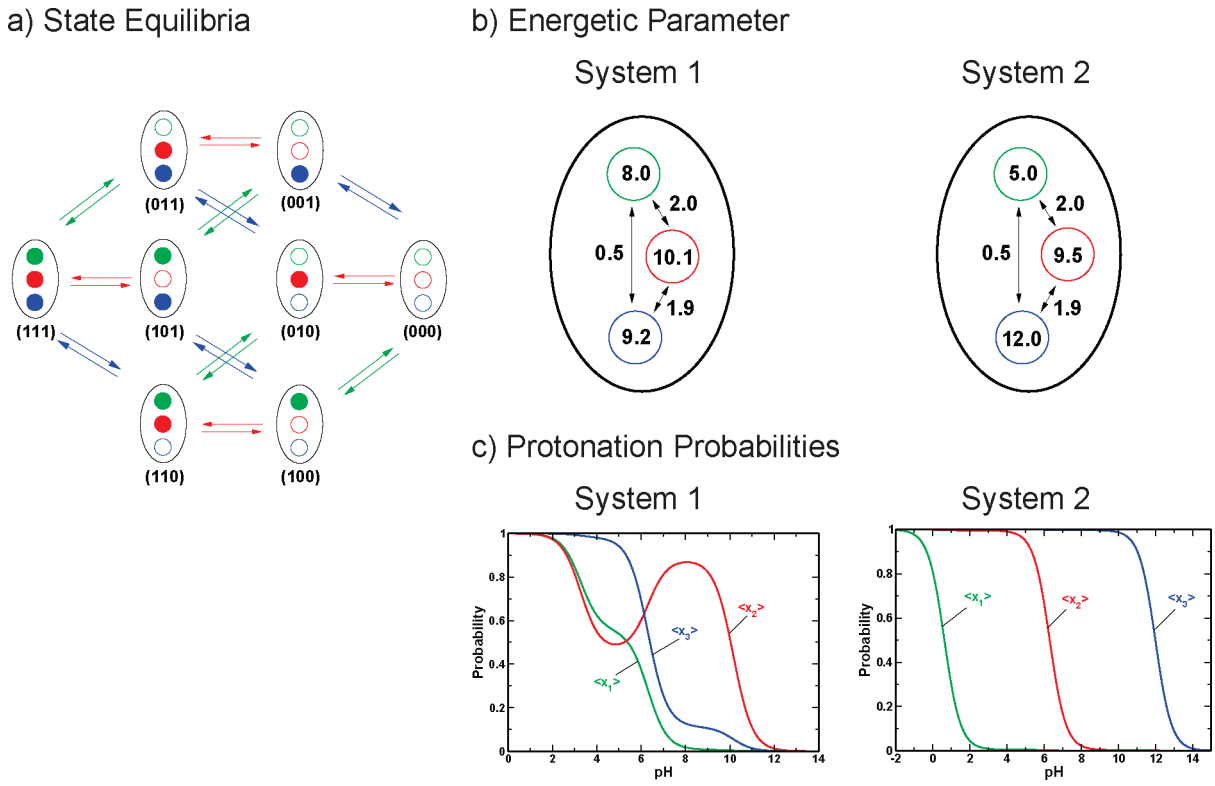

Figure 3. (a) State equilibria of a system with three titratable sites. Eight protonation microstates exist for such a system. The protonation state vectors are given in parentheses. (b) Energetic parameters of the two discussed systems. The numbers inside the circles give the pK_{intr} values, and the numbers at the arrows give the interaction energy of the protonated species in pK_a units. (c) Titration curves of the individual sites (protonation probabilities) for system 1 and system 2. The colors in all graphs and schemes are associated with the corresponding sites (green for site 1; red for site 2; blue for site 3).

and 6.5 for the two sites. If the pK_a values of the individual sites, HH-pK_a and TR-pK_a (Figure 2d), are calculated, one sees that they depend on pH. This finding is not too surprising because of the irregular titration curves. As can be seen from the pK_a plot (Figure 2d), both the HH-pK_a and the TR-pK_a values vary between the microscopic pK_a values (dashed-dotted lines) that are associated with the deprotonation of the respective site (red arrows for site 1 and blue arrows for site 2 in Figure 2a). The protonation free energy can be read from the difference between the bisection line (dotted line in Figure 2d, pK_a = pH) and the respective pK_a curves (see Figure 1). The pH dependence of the protonation free energy is given in Figure 2e. The absolute value of the free energy difference calculated from the HH-pK_a value tends to be similar or smaller than the absolute value of the free energy difference calculated from TR-pK_a value. This finding can be explained by the fact that the additional relaxation of the protonation of the surrounding residues, which is included in the HH-pK_a value but not in the TR-pK_a value, lowers the free energy difference.

An important finding is that the absolute free energy difference for changing the protonation of the sites (solid and dashed lines in Figure 2e calculated from the HH-pK_a and the TR-pK_a value, respectively) is varying between the values that are obtained from the microscopic pK_a values associated with this site (dashed-dotted lines in Figure 2e). The protonation energy of one site in the discussed system of two interacting sites has the magnitude of thermal energy at room temperature (0.6 kcal/mol) or less over a range of 2.5 pH units (Figure 2e). For an isolated protonatable site, this free energy difference is in the thermal energy range only over a range of about 1.0 pH unit. Thus, due to the interaction between the sites, the protonated and deprotonated forms of the sites are close in energy over a wide pH range enabling a less pH-sensitive catalytic function.

Next we consider two interacting sites that titrate at a different pH range (system 2 in Figure 2). We set the intrinsic pK_a values to 4.0 and 7.0, which, due to the interaction energy of 2.0 pK_a units, results in the following microscopic pK_a values: pK_{11}^{10} = 5.0, pK_{11}^{01} = 2.0, pK_{01}^{00} = 7.0, and pK_{10}^{00} = 4.0. The titration curves of the two sites look like standard sigmoidal titration curves that are described by Henderson−Hasselbalch titration curves with pK_a values of 2.0 and 7.0 (Figure 2f). However, if the HH- and TR-pK_a values are calculated, one sees that also for this system, the individual site pK_a values vary with pH (Figure 2g). When site 2 titrates from pH 4 to 8 (blue curve in Figure 2f), site 1 changes its pK_a value from 2 to 4 (red curve in Figure 2g). Therefore, suppose site 1 would accept transiently a proton during a catalytic step at pH = 8; the pK_a value connected to this reaction is about 4 even if the titration curve has its midpoint at pH = 2. Thus, the energy required to protonate this group at pH = 8 is according to eq 1 about 5.5 kcal/mol instead of 8.2 kcal/mol, which would correspond to a protonation energy of a group with the pK_a value of 2.0 (Figure 2h). In the pH range from 5 to 7, the solid curve in Figure 2h displays a plateau indicating that the energy required to protonate site 1 is nearly constant. Thus, interactions between protonatable residues in proteins can tune protonation energies of a site and keep this energy constant over a pH range that is wider than the range expected from the titration curve of this site. This aspect is put in evidence by introducing individual site pK_a values.

System with Three Sites. Three interacting sites can lead to an even more complex titration behavior. In this case, titration curves may be also nonmonotonic as for example for DTPA.[3]

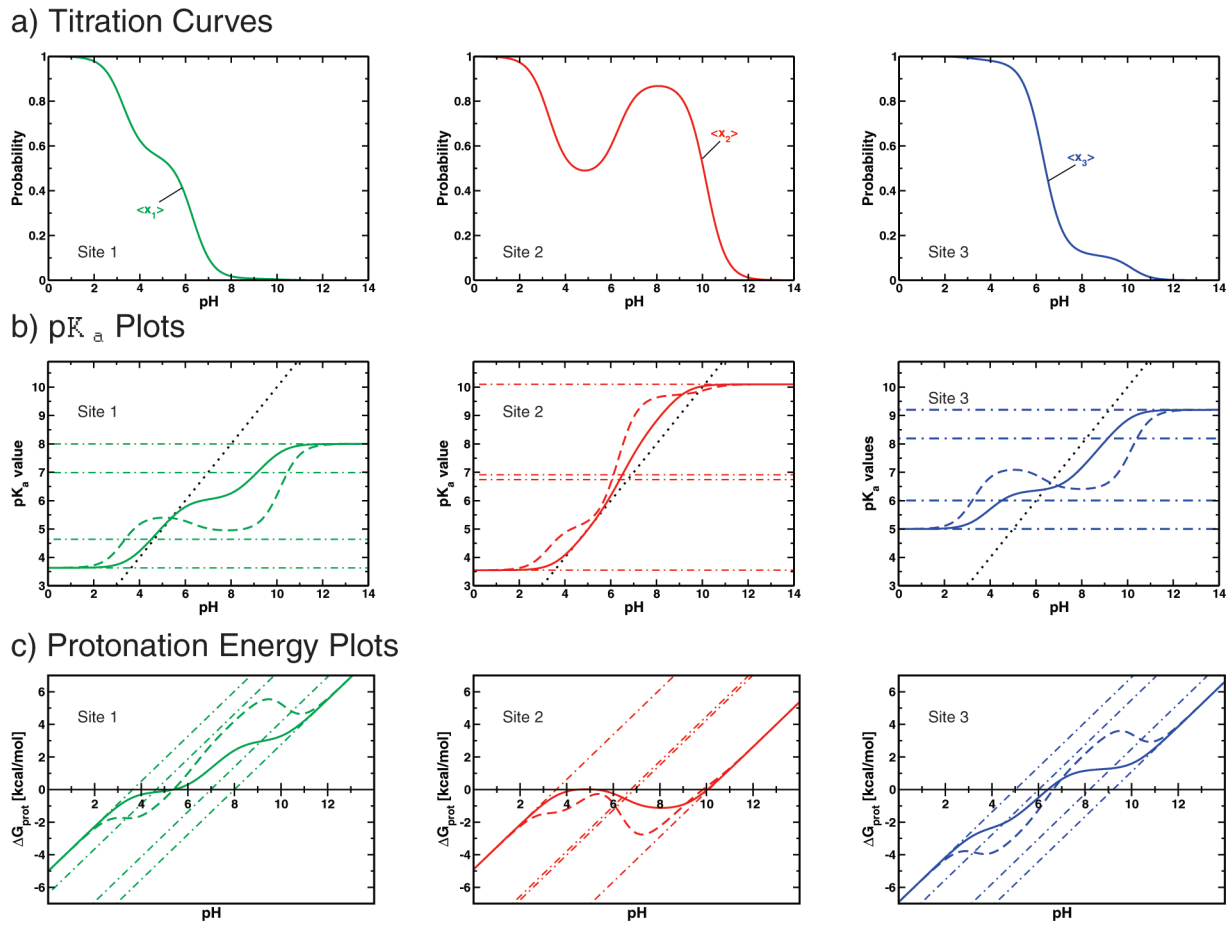

Figure 4. Titation curves (a), pK_a plots (b), and protonation energy plots (c) of the three sites of system 1 of Figure 3. The energetic parameters of this system are defined in Figure 3b. The titration curves are the same as in Figure 3c. The pK_a plots (b) shows differently defined pK_a values: HH-pK_a (solid), TR-pK_a (dashed), microscopic pK_a (dashed-dotted), and the bisection line pH = pK_a (dotted line). The protonation free energies are calculated from eq 1 for the differently defined pK_a values (same coding as above). The colors in all graphs and schemes are associated with the corresponding sites (green for site 1; red for site 2; blue for site 3).

Nevertheless, the basic features of the titration behavior still remain the same.

In Figure 3, two systems of three interacting sites are depicted. Both systems have the same set of interaction energies between the sites. They differ in the intrinsic pK_a values of the sites (Figure 3b). Here again the fully deprotonated state is considered as the reference state.

In system 1, the three sites titrate in the same pH range. The interaction between the sites keeps the protonation free energy low over a wide pH range. Especially the site with the most irregular titration curve (red curve in Figure 3c and Figure 4a) has a HH-pK_a value that is almost identical with the pH over a wide pH range (red curve in Figure 4b). In particular, the small difference between the HH-pK_a value and the pH value implies that the protonation energy for this site is particularly low over this pH range (Figure 4c). The pK_a values of each individual site vary between the most extreme microscopic pK_a values associated with the deprotonation of the respective site (Figure 4b). Usually, the minimal microscopic pK_a value corresponds to the pK_a value that the site would have if all other sites are protonated, and the maximal microscopic pK_a value corresponds to the pK_a value that the site would have if all other sites are deprotonated.

In system 2, the three sites titrate at separate pH values (Figure 3c). Although their titration curves resemble standard sigmoidal titration curves (Figure 5a), the pK_a values of the individual sites depend on pH (Figure 5b). In this system, none of the sites has a pK_a value that is close to the pH value over a wide pH range. However, for all sites, there are certain pH ranges in which the slope of the pH dependence of the pK_a value is close to one; i.e., the pH dependence of the pK_a value is parallel to the line pK_a = pH. This interesting feature implies that the protonation energy is nearly constant over those pH ranges. Also for this system, the pK_a values of the individual sites vary between the most extreme microscopic pK_a values associated with the deprotonation of the respective site (Figure 5b). It can be seen that each site has an individual pK_a value that coincides with one of its microscopic pK_a values in the pH range in which none of the other sites is titrating (see, for example, in Figure 5b the solid green curve in the pH ranges from −2 to 2, from 8 to 10, and from 13 to 15).

Plastocyanin. Plastocyanin is a small electron-transfer protein. A large negatively charged surface region, called an acidic patch, is involved in the interaction with its reaction partners. This acidic patch can be divided into an upper acidic patch and a lower acidic patch (see Figure 6a). Using electrostatic calculations, the titration curves of the amino acids of the acidic patch were determined and correlated with experimental data.[22] By chance, Glu45 (in the lower acidic patch) and Glu59 (in the upper acidic patch) have very similar titration curves, and the midpoint of their titration curves (i.e., their p$K_{1/2}$) is the same (Figure 6b). Moreover, both curves are similar to a standard HH curve with a pK_a value of 4.95. However, the individual site pK_a values (HH-pK_a and TR-pK_a) show a strong pH

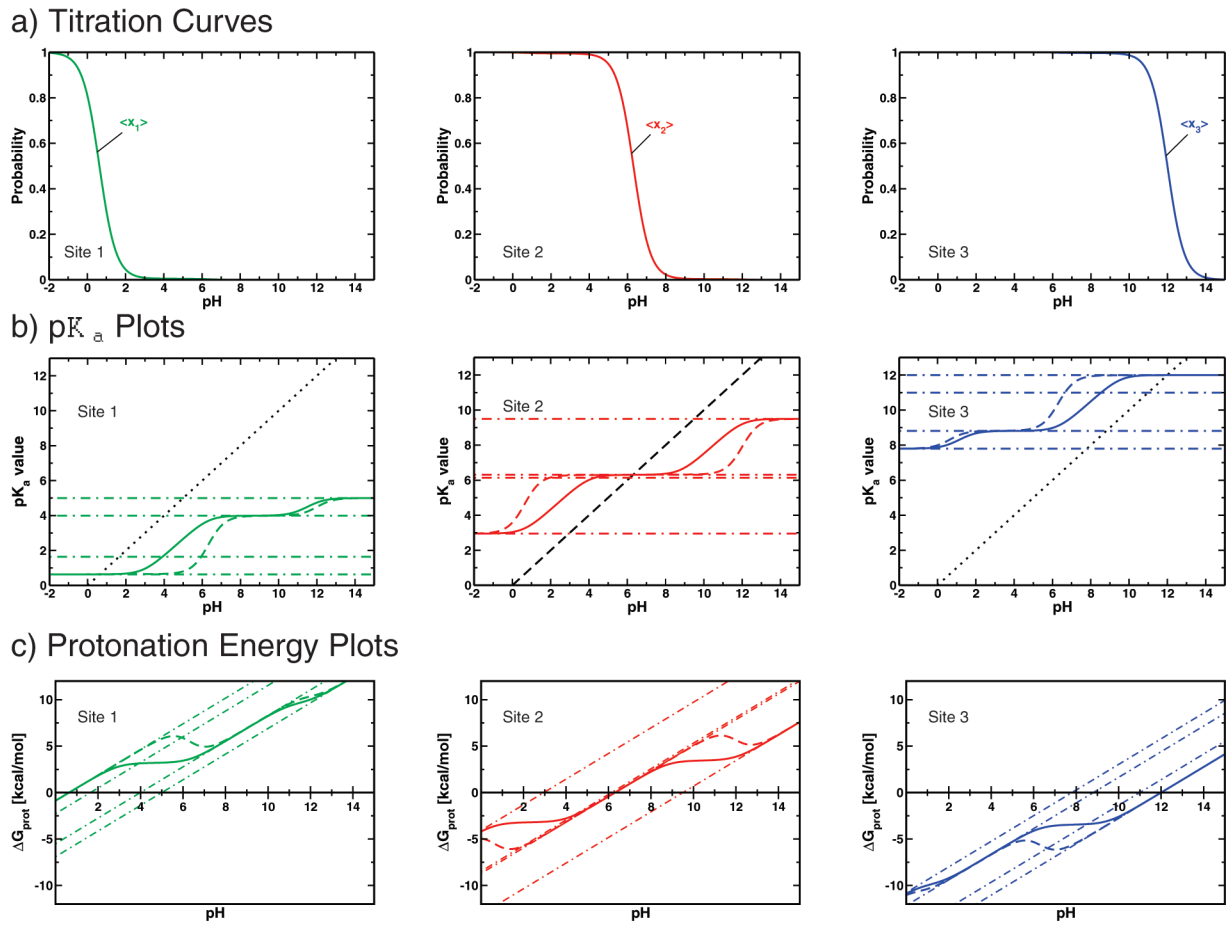

Figure 5. Titation curves (a), pK_a plots (b), and protonation energy plots (c) of the three sites of system 2 of Figure 3. The energetic parameters of this system are defined in Figure 3b. The titration curves are the same as in Figure 3c. The pK_a plots (b) shows differently defined pK_a values: HH-pK_a (solid), TR-pK_a (dashed), microscopic pK_a (dashed-dotted), and the bisection line pH = pK_a (dotted line). The protonation free energies are calculated from eq 1 for the differently defined pK_a values (same coding as above). The colors in all graphs and schemes are associated with the corresponding sites (green for site 1; red for site 2; blue for site 3).

dependence, and this pH dependence is significantly different for Glu45 and Glu59 despite their similar titration curves (Figure 6c). The different pH dependence of the individual site pK_a values of the two residues shows that these residues have different electrostatic interactions with other titratable residues of the protein. This result would have been overlooked if only the titration curves instead of the pH dependence of the individual site pK_a values would have been analyzed.

RNase T1. Finally, we are considering the enzyme RNase T1[23] which performs the hydrolytic cleavage of RNA by acid−base catalysis. The residue Glu58 functions as a proton acceptor in the first step of the catalytic cycle (Figure 7a). Electrostatic calculations of the titration curves of Glu58 using the same settings as in previous calculations[26] indicate that this residue titrates at a rather low pH (Figure 7b). The p$K_{1/2}$ value of this titration curve is 1.65. The titration curve of this residue does not deviate largely from a standard HH curve; in fact, the low protonation probability above pH = 4 is probably not detectable experimentally. Despite this apparent standard titration curve, the HH-pK_a and the TR-pK_a show a strong pH dependence (Figure 7c). The protonation free energy deviates largely from the value that would have been calculated considering the p$K_{1/2}$ value of the titration curve (Figure 7d). If the protonation free energy of this residue is calculated from the HH-pK_a value, it is practically constant from pH 4 to 8 (see solid curve in Figure 7d). The free energy calculated from the TR-pK_a value is not identical with the one calculated from the HH-pK_a value, since the relaxation of the protonation of the surrounding residues is not considered. Anyway, the protonation free energies calculated both from the HH-pK_a value and from the TR-pK_a value differ considerably from the linear pH dependence that would have been obtained using the p$K_{1/2}$ value. Again, this behavior is a consequence of the electrostatic interaction of Glu58 with other titratable residues of the protein, especially with His40 and His92. This example demonstrates that p$K_{1/2}$ values determined from titration curves may be misleading and do not necessarily reflect the correct energetics of protonation reactions in proteins. In contrast, the use of individual pK_a values allows one to pinpoint important features.

Conclusions

Although it is a common praxis to read pK_a values of amino acids in proteins from titration curves measured by NMR, FTIR, or other methods and to infer the protonation free energies from these pK_a values, we showed in this article that this strategy cannot be generally followed. Indeed, we demonstrate that the complex interaction between protonatable sites in the protein make protonation energies nonlinearly dependent on pH. This behavior can be described by defining pH-dependent pK_a values for individual sites in a protein. Even if the titration curve of a residue in a protein shows an apparently standard sigmoidal shape that obeys the Henderson−Hasselbalch equation, the protonation energy of such a residue may show a much more

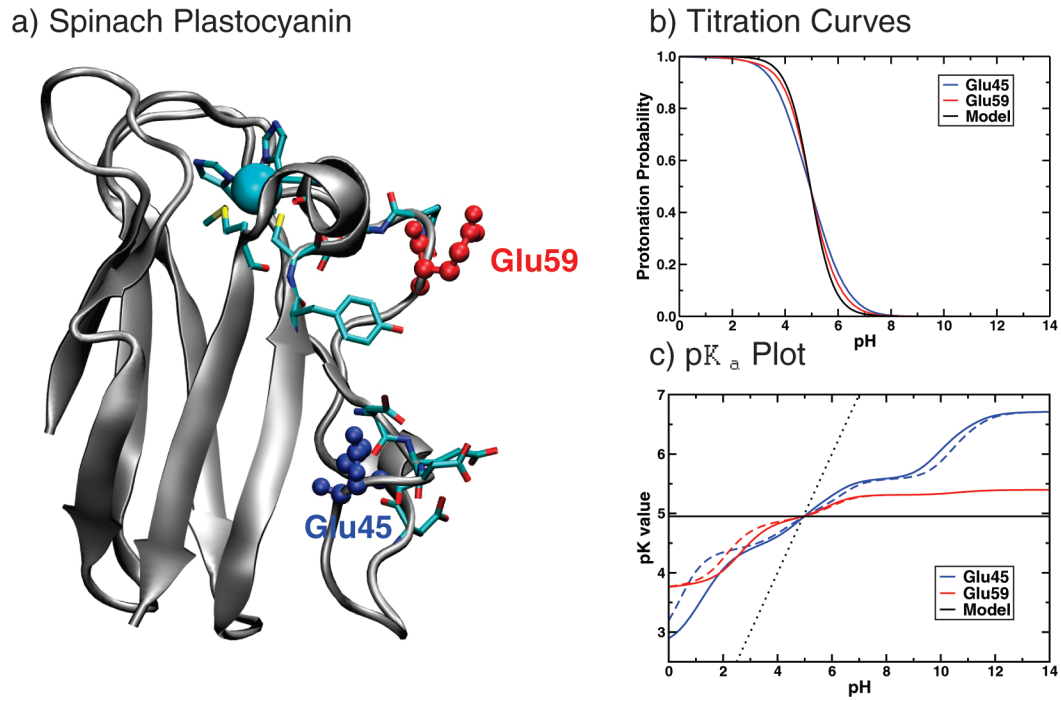

Figure 6. Titration behavior of two residues in spinach plastocyanin. (a) Structural representation of spinach plastocyanin (PDB code 1AG6). The residues Glu45 and Glu59 are shown as blue and red ball-and-stick models, repectively. The copper ion (cyan sphere), its ligands, and Tyr83 (on the right in the middle) are given as an orientation. Also the additional negatively charged residues of the acidic patch are shown. (b) Titration curves of Glu45 (blue) and Glu59 (red). For comparison, a standard HH titration curve with a pK_a of 4.95 is given (black). (c) Differently defined pK_a values for Glu45 (blue), Glu59 (red): HH-pK_a (solid), TR-pK_a (dashed), microscopic pK_a (dashed-dotted), and the bisection line pH = pK_a (dotted line).

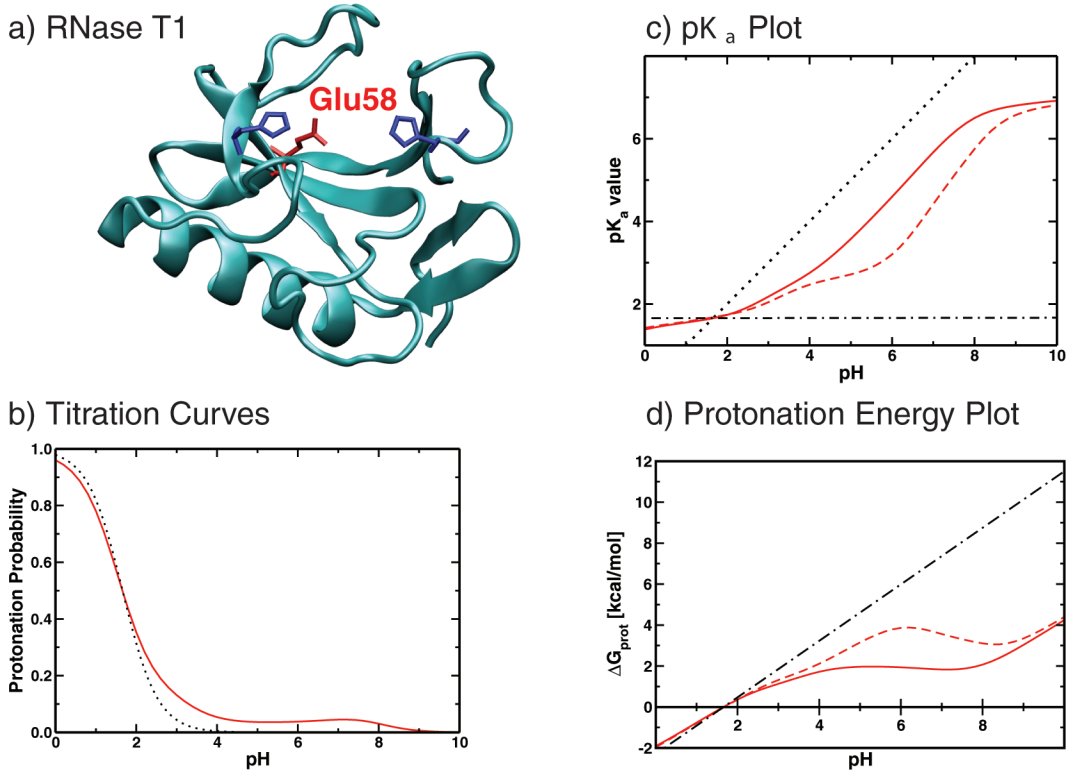

Figure 7. (a) Structural representation of RNase T1 (PDB code 1BVI, chain A). The catalytically active residue Glu58 is shown in red. The two strongly interacting residues His40 and His92 are shown in blue. (b) Calculated titration curve of Glu58 (without the substrate present). For comparison, a standard HH titration curve with a pK_a of 1.65 is given (black). (c) Differently defined pK_a values for Glu58: HH-pK_a (solid), TR-pK_a (dashed). The dotted line is the bisection line pH = pK_a. The black dashed-dotted line represents a pH-independent pK_a value of 1.65. (d) Protonation free energies of Glu58 calculated from eq 1 for the different pK_a values. The black dashed-dotted curves gives the protonation energy of a site with a pK_a value of 1.65.

complex pH dependence than the titration curve indicates. The use of pH-dependent pK_a values for individual sites allows one to reveal that the interaction with other titratable sites may lead to constant protonation energy over a large pH range. Biologi-

cally it may be important that the protonation energy of a particular residue that functions as proton donor or acceptor is constant over a large pH range in order to allow catalysis under different pH conditions. In this frame, we can understand why in the active site of enzymes there are often more protonatable residues than the specific function would require.

In this paper, we discuss proton binding to proteins. However, the same statements are obviously valid also for nucleic acids, lipid membranes, and all other kind of natural or synthetic polyelectrolyes and their aggregates. Instead of protons, other kind of ligands can be considered such as electrons, ions, or even more complex molecules.

From this analysis, we conclude that the energetics of binding to one particular binding site can generally not be understood solely from titration curves. Concerted efforts of thermodynamic, kinetic, spectroscopic, and structural investigations combined with a detailed theoretical analysis are required to understand these reactions.

Acknowledgment. This work was supported by the DFG grant UL174/7-1. E.B. is funded by a Marie-Curie-Intraeuropean Fellowship (MEIF-CT-2006-023403). We thank Dr. Timm Essigke for useful discussions.

References and Notes

(1) Bashford, D.; Case, D. A.; Dalvit, C.; Tennant, L.; Wright, P. E. Electrostatic Calculations of Side-Chain pK_a Values in Myoglobin and Comparisation with NMR Data for Histidines. *Biochemistry* **1993**, *32*, 8045–8056.

(2) Bashford, D.; Karplus, M. Multiple-Site Titration Curves of Proteins: An Analysis of Exact and Approximate Methods for Their Calculations. *J. Phys. Chem.* **1991**, *95*, 9557–9561.

(3) Sudmeier, J. L.; Reilley, C. N. Nuclear Magnetic Resonance Studies of Protonation of Polyamine and Aminocarboxylate Compounds in Aqueous Solution. *Anal. Chem.* **1964**, *36*, 1698–1706.

(4) Bombarda, E.; Morellet, N.; Cherradi, H.; Spiess, B.; Bouaziz, S.; Grell, E.; Roques, B. P.; Mely, Y. Determination of the pK_a of the Four Zn^{2+}-Coordinating Residues of the Distal Finger Motif of the HIV-1 Nucleocapsid Protein: Consequences on the Binding of Zn^{2+}. *J. Mol. Biol.* **2001**, *310*, 659–672.

(5) Onufriev, A.; Case, D. A.; Ullmann, G. M. A Novel View on the pH Titration of Biomolecules. *Biochemistry* **2001**, *40*, 3413–3419.

(6) Ullmann, G. M. Relations between Protonation Constants and Titration Curves in Polyprotic Acids: A Critical View. *J. Phys. Chem. B* **2003**, *107*, 1263–1271.

(7) Klingen, A. R.; Bombarda, E.; Ullmann, G. M. Theoretical Investigation of the Behavior of Titratable Groups in Proteins. *Photochem. Photobiol. Sci.* **2006**, *5*, 588–596.

(8) Bashford, D.; Karplus, M. pK_a's of Ionizable Groups in Proteins: Atomic Detail from a Continuum Electrostatic Model. *Biochemistry* **1990**, *29*, 10219–10225.

(9) Sham, Y. Y.; Chu, Z. T.; Warshel, A. Consistent Calculation of pK_a's of Ionizable Residues in Proteins: Semi-mircoscopic and Microscopic Approaches. *J. Phys. Chem. B* **1997**, *101*, 4458–4472.

(10) Ullmann, G. M.; Knapp, E. W. Electrostatic Computations of Protonation and Redox Equilibria in Proteins. *Eur. Biophys. J.* **1999**, *28*, 533–551.

(11) Gunner, M.; Alexov, E. A Pragmatic Approach to Structure Based Calculation of Coupled Proton and Electron Transfer in Proteins. *Biochim. Biophys. Acta* **2000**, *1458*, 63–87.

(12) Beroza, P.; Fredkin, D. R.; Okamura, M. Y.; Feher, G. Protonation of Interacting Residues in a Protein by a Monte Carlo Method: Application to Lysozyme and the Photosynthetic Reaction Center. *Proc. Natl. Acad. Sci. U.S.A.* **1991**, *88*, 5804–5808.

(13) Klotz, I. M. *Ligand-Rezeptor Energetics*; Wiley & Sons Inc.: New York, 1997.

(14) Tanford, C.; Roxby, R. Interpretation of Protein Titration Curves. Application to Lysozyme. *Biochemistry* **1972**, *11*, 2192–2198.

(15) Homeyer, N.; Essigke, T.; Ullmann, G. M.; Sticht, H. Effects of Histidine Protonation and Phosphorylation on HPr Structure, Dynamics and Physicochemical Properties. *Biochemistry* **2007**, *46*, 12314–12326.

(16) Xue, J.; Okvist, M.; Hansson, O.; Young, S. Crystal Structure of Spinach Plastocyanin at 1.7 Å Resolution. *Protein Sci.* **1998**, *7*, 2099–2105.

(17) Langhorst, U.; Loris, R.; Denisov, V. P.; Doumen, J.; Roose, P.; Maes, D.; Halle, B.; Steyaert, J. Dissection of the Structural and Functional Role of a Conserved Hydration Site in RNase T1. *Protein Sci.* **1999**, *8*, 722–730.

(18) Brooks, B. R.; Bruccoleri, R. E.; Olafson, B. D.; States, D. J.; Swaminathan, S.; Karplus, M. CHARMM: A Program for Macromolecular Energy, Minimization, and Dynamics Calculation. *J. Comput. Chem.* **1983**, *4*, 187–217.

(19) Bashford, D.; Gerwert, K. Electrostatic Calculations of the pK_a Values of Ionizable Groups in Bacteriorhodopsin. *J. Mol. Biol.* **1992**, *224*, 473–486.

(20) MacKerell, A. D.; Bashford, D.; Bellott, M.; Dunbrack, R. L., Jr.; Evanseck, J. D.; Field, M. J.; Fischer, S.; Gao, J.; Guo, H.; Ha, S.; Joseph-McCarthy, D.; Kuchnir, L.; Kuczera, K.; Lau, F. T. K.; Mattos, C.; Michnick, S.; Ngo, T.; Nguyen, D. T.; Prodhom, B.; Reiher, W. E.; Roux, B.; Schlenkrich, M.; Smith, J. C.; Stote, R.; Straub, J.; Watanabe, M.; Wiorkiewicz-Kuczera, J.; Yin, D.; Karplus, M. All-Atom Empirical Potential for Molecular Modeling and Dynamics Studies of Proteins. *J. Phys. Chem. B* **1998**, *102*, 3586–3616.

(21) Klapper, I.; Fine, R.; Sharp, K. A.; Honig, B. H. Focusing of Electric Fields in the Active Site of Cu−Zn Superoxide Dismuatase: Effects of Ionic Strength and Amino-Acid Modification. *Proteins* **1986**, *1*, 47–59.

(22) Crnogorac, M.; Ullmann, G. M.; Kostić, N. M. Effects of pH on Protein Association. Modification of the Proton Linkage Model and Experimental Verification of the Modified Model in the Case of Cytochrome c and Plastocyanin. *J. Am. Chem. Soc.* **2001**, *123*, 10789–10798.

(23) Pace, C. N.; Heinemann, U.; Hahn, U.; Saenger, W. Ribonuclease T1: Structure, Function, and Stability. *Angew. Chem., Int. Ed. Engl.* **1991**, *30*, 343–360.

(24) Rabenstein, B.; Ullmann, G. M.; Knapp, E. W. Energetics of the Electron Transfer and Protonation Reactions of the Quinones in the Photosynthetic Reaction Center of *Rhodopseudomonas viridis*. *Biochemistry* **1998**, *37*, 2488–2495.

(25) Calimet, N.; Ullmann, G. M. The Influence of a Transmembrane pH Gradient on Protonation Probabilities of Bacteriorhodopsin: The Structural Basis of the Back-Pressure Effect. *J. Mol. Biol.* **2004**, *339*, 571–589.

(26) Bombarda, E.; Becker, T.; Ullmann, G. M. The Influence of the Membrane Potential on the Protonation of Bacteriorhodopsin: Insights from Electrostatic Calculations into the Regulation of Proton Pumping. *J. Am. Chem. Soc.* **2006**, *128*, 12129–12139.

JP908926W